Efficient method for Li doping of α-rhombohedral boron

H. Dekura,* K. Shirai,† and A. Yanase

Nanoscience and Nanotechnology Center, Institute of Scientific and Industrial Research (ISIR), Osaka University, 8-1 Mihogaoka, Ibaraki, Osaka 567-0047, Japan

(Received 5 May 2011; revised manuscript received 10 August 2011; published 23 September 2011)

Li doping is a promising method for achieving metallization of α-rhombohedral boron (α-boron for short), which is a potential candidate for a high-T_c superconducting material. Toward this end, a serious drawback has been the difficulty of doping α-boron, even though there are theoretical predictions claiming that it should be easy. This discrepancy has been systematically studied by the *ab initio* pseudopotential method through calculations of various structural and phonon properties of the material. For this study, a comparison with β-boron is important because experimental data are available in this case. The present results demonstrate that while Li doping is difficult for α-boron under normal conditions, it is easy for β-boron, which is completely consistent with experiments. The difference between these crystals originates from the contrasting characteristics of the bonding. For α-boron, the bonding requirement of the host crystal is fulfilled so well that the only way for a Li atom to enter the crystal is through the antibonding states. Electronically, this is favorable because it causes an almost perfect rigid-band shift without modifying the bonding nature of the host crystal. In terms of structural effects, Li doping causes a slight decrease in the cell angle α_{rh} as well as softening of the elastic properties. A striking effect of Li doping is manifested in substantial phonon softening of the librational mode. These changes can be regarded as reliable criteria for the experimental detection of Li inclusion. On the other hand, β-boron can be characterized as a frustrated system, and the crystal has a propensity to welcome guest atoms in order to eliminate ill-connected bonds. As a result, even though Li is easily incorporated into β-boron, the carriers are not activated for electrical conduction. The remaining problem is how to overcome the difficulty of Li doping of α-boron. The most important contribution of this study lies in demonstrating the usefulness of high-pressure synthesis as an efficient doping method.

DOI: 10.1103/PhysRevB.84.094117 PACS number(s): 81.05.Cy, 61.72.Bb, 71.55.Cn

I. INTRODUCTION

Since the beginning of the 21st century, there have been considerable breakthroughs in the field of superconductivity in semiconductors. The first breakthrough appeared in the superconductivity of β-boron at high pressure ($T_c \sim 5$ K at $p = 160$ GPa, increases together with pressure), which was demonstrated by Eremets in 2001.[1] Although the crystal structure was not identified well at the time, this discovery attracted the interest of many researchers in high-T_c superconducting materials. For example, there is a theoretical calculation showing that $T_c \geqslant 50$ K at extreme pressure.[2] The second breakthrough concerns heavy doping performed in order to achieve metal-insulator transitions. Ekimov *et al.* first showed the occurrence of superconducting transition in heavily B-doped diamond.[3] Immediately, this technique was applied to other semiconductors. As a result, we are currently witnessing an expanding list of heavily doped semiconductors exhibiting superconductivity, such as Si,[4,5] SiC,[6] and InN.

Collaborating with Japanese experimentalists, we have been studying the superconductivity of α-rhombohedral boron (hereinafter abbreviated simply as α-boron) because of its potential for use in high-T_c materials.[7] The recent discovery of superconductivity in α-boron is a notable result of our collaboration: Superconductivity appears at $\sim$160 GPa with $T_c \sim 5$ K.[8] Although the critical temperature is almost the same as that of β-boron, this discovery entailed a number of scientific contributions. If we had conducted similar studies on β-boron, we would have been unable to reach this level of progress. In this regard, the mechanism of the metallization under pressure has been clarified.[9,10] An anomaly reported in resistivity measurement at high pressure, that is, a kink in the pressure dependence of resistivity, has been attributed to electronic band bowing caused by structural change manifested in an altered cell angle. This theoretical development was possible only as a result of the simplicity of the crystal structure of α-boron and its stability at high pressure. Another (technologically more important) merit of considering α-boron is its defect-free structure. Most boron-rich crystals other than α-boron contain a considerable amount of defects yielding electronic gap states,[11] and it is believed that the electrical conduction mechanism is based on the hopping between defect sites.[12–16] This makes it difficult to control the valence electrons by doping. Recent theoretical studies have proven that this feature is intrinsic; in other words, it is not caused by the entropic contribution at finite temperatures, but is rather a property of the ground state.[17–21] Only for α-boron is the conduction in accordance with the standard mechanism of band conduction.[9]

Although the discovery of superconductivity in boron has entailed great contributions to science, extremely high pressures, such as 160 GPa, are highly demanding for industrial applications. This is one reason for applying carrier doping, and the naturally defect-free structure of α-boron is fully usable for this purpose. The idea of doping boron is not new. It was proposed some 15 years ago by Gunji and Kamimura in analogy to doped C_{60}.[22] Among various candidates for dopants, they pointed out that the most appropriate one would be Li based on chemical trends related to ionic radius. At present, by performing first-principles calculations, we are able to find the most appropriate impurities in terms of formation energy. Over a wide range of impurities (a few of them are

presented in our conference proceedings[23]), our calculations show that the pioneering work of Gunji and Kamimura is still correct in that Li is the most appropriate dopant in terms of both formation energy and rigid-band shift.[24] However, we found inconsistencies in certain numerical values.[23] Our results regarding the sign of the formation energy implies that Li doping is likely to be difficult, which contradicts previous studies.[22,25–27] After deducing that Li doping is easy in terms of formation energy, Hayami argued that the actual difficulties related to doping arise in the diffusion process in solid boron.[26] By considering the increasing importance of doping in the research of superconductivity, this discrepancy cannot be overlooked. Although there have been extensive efforts to develop an efficient method for doping Li to α-boron, there has been no marked success.[28] On the other hand, although doping of β-boron has been successful, metallic properties have, to the best of our knowledge, unfortunately never been observed.[29,30] Therefore, it is necessary to investigate the reasons why successful doping has been achieved for β-boron and not for α-boron even though their respective structures are similar.

In this paper, we systematically investigated Li doping of α-boron, and we not only resolved the problem of the formation energy, but also clarified many structural characteristics that have not been carefully analyzed in previous studies.[22,26] In addition, the present calculations cover the issue of Li-doped β-boron. A comparison with β-boron is particularly important since experimental data are available for only this polymorph.[29,30] The various means of comparison can provide confirmation of the present calculations, and more importantly, the paper offers useful predictions for the structural changes in Li-doped α-boron, which are good guidelines for experimental detection of Li incorporation.

Based on these considerations, we conclude that Li doping is difficult to perform for α-boron when using solid Li and B, which might discourage experimentalists from performing doping. Another aim of the present theoretical paper is to propose a way to overcome such difficulties through material design. In attempting to overcome this difficulty by a trial-and-error approach, we have devised an efficient method of high-pressure synthesis. The discussion of this issue, which is the most important contribution of this work, is presented in the last section of this paper.

II. METHOD

A. Theoretical background

Note that the term "formation energy," which is denoted as ΔE_f, is used differently in different areas, for example, in alloy systems and impurity systems. Yet there is no interference as long as it is discussed separately. However, in the literature pertaining to heavily doped semiconductors, confusion arises with regard to this term. Although for fullerides, intercalated compounds, and clathrates, doped materials are often referred to as impurity systems, some of them are compounds in the strict sense. This is true also in the present study: Li-doped α-boron and Li-doped β-boron are in fact compounds. Since the present argument traverses a wide range of compositions of foreign atoms, some notes on the formation energy are needed at the outset.

In impurity systems, ΔE_f is defined as the energy required to incorporate an impurity atom B into the host crystal A. In density-functional theory (DFT) calculations performed by using an n-atom supercell, it is calculated as

$$\Delta E_f = E(\mathrm{A}_n\mathrm{B}) - \{nE(\mathrm{A}) + E(\mathrm{B})\}. \quad (1)$$

In actual calculations, n is taken to be as large as practically possible. By defining it in this way, ΔE_f becomes positive, and accordingly only a small fraction of impurity atoms can be incorporated into the host crystal. A positive ΔE_f determines the concentration c of impurities at a finite temperature T through $c \sim \exp(-\Delta E_f/kT)$, where k is the Boltzmann constant. On the other hand, in alloy systems, ΔE_f is defined as the energy gain necessary for forming an alloy $\mathrm{A}_{1-x}\mathrm{B}_x$ from its constituents:

$$\Delta E_f = \{(1-x)E(\mathrm{A}) + xE(\mathrm{B})\} - E(\mathrm{A}_{1-x}\mathrm{B}_x). \quad (2)$$

Note that the sign is opposite to that in Eq. (1). Also, the energy is evaluated as a quantity which is averaged per atom (or molar quantity). In this case, ΔE_f for a particular composition x alone does not guarantee the stability of an alloy $\mathrm{A}_{1-x}\mathrm{B}_x$. By knowing ΔE_f for all possible candidates having different compositions, we can determine the phase diagram of the alloy system $\mathrm{A}_{1-x}\mathrm{B}_x$.[31] When a positive ΔE_f is obtained for a composition x, we can say only that there must be a stable alloy somewhere between $0 < x < 1$.

Here, we follow the sign convention of Eq. (1) throughout the paper, regardless of whether it refers to an impurity or an alloy. However, ΔE_f is evaluated either as the energy per impurity atom or per constitution atom, as most suitable to the specific problem at hand. For solid-state reactions, evaluation of the formation energy ΔE_f is usually enough for judging whether or not the reaction proceeds. However, for high pressure, the effect of volume change must be taken into account, which is done by evaluating the formation enthalpy ΔH_f.

Another related issue is the site occupancy. In impurity systems, the site of an impurity is only partially occupied owing to randomness. On the other hand, in stoichiometric compounds, even guest atoms must have perfect occupancy at specific sites. For α-boron, there is no experimental information about the impurity sites, because of experimental difficulty for sample preparation. We use a structure of perfect occupancy LiB_{12} as a structural model for doped α-boron. Although we have already performed supercell calculations for lower Li concentrations, only the results of perfect occupancy LiB_{12} are relevant in the present context. For β-boron, the situation is more complicated. Even for nondoped β-boron, there are sites with partial occupancy. Because of both the computational load and of our ability of understanding, we use a perfect structure $\mathrm{Li}_8\mathrm{B}_{105}$ as the structural model. Details of impurity sites of β-boron is described in Sec. III C.

B. Calculation method

Density-functional calculations were performed to obtain the total energy and to determine the crystal structure doped with Li. In this paper, the plane-wave and norm-conserved

pseudopotential methods were used with the aid of the OSAKA2K (Ref. 32) and QUANTUM ESPRESSO (Ref. 33) software packages. The parametrized form of the local-density approximation (LDA), as proposed by Perdew and Zunger,[34] and the PBE form of the generalized gradient approximation (GGA) were used for the exchange-correlation term.[35] The Troullier-Martins pseudopotential[36] was used with the aid of a fully separable Kleinman-Bylander form.[37] Initially, a nonlinear core correction was implemented for both B and Li atoms. However, we found that it had no significant change with respect to the energy, and therefore we do not include this correction in the present study. Plane waves were expanded with a kinetic cutoff energy of 70 Ry, and $6 \times 6 \times 6$ and $10 \times 10 \times 10$ Mohkhorst-Pack k grids were applied for nondoped and Li-doped α-boron, respectively. Structural optimization was performed with residual force of less than 10^{-5} Ry/Bohr and a residual stress of less than 0.01 GPa. The convergence of the above conditions was thoroughly tested in previous studies.[17,38]

The formation enthalpy ΔH_f was obtained by adding pV term to ΔE_f, where V is the volume of the crystal. The volume V was determined as a function of p in the structural optimization. Furthermore, density-functional perturbation technique was applied for the calculation of phonon eigenvectors and eigenfrequencies.[39] In this case, a k mesh of $10 \times 10 \times 10$ was necessary in order to obtain a reasonable resolution. Here, only zone center modes are discussed.

III. Li DOPING

A. Formation energy

Among the O, T, and I impurity sites as indicated in Fig. 1, the most stable one is the O site. This has been first

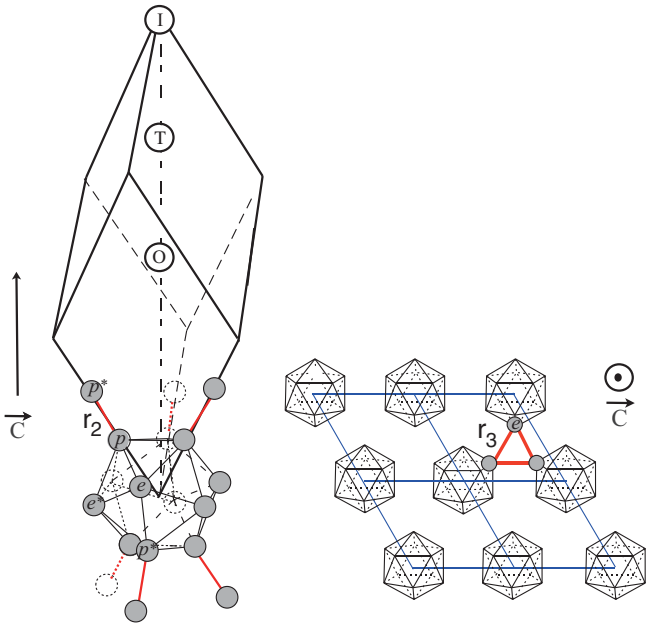

FIG. 1. (Color online) The crystal structure of α-boron with O, T, and I impurity sites. These impurity sites are located on the main diagonal of the rhombohedral unit cell. Intericosahedral p-p^* and e-e bonds denoted as r_2 and r_3, respectively, are shown in this figure.

demonstrated by Gunji and Kamimura,[22] and it represents the point upon which all of the published studies,[22,26] including the present paper, agree. In the present calculations, relative to the O site, the formation energy ΔE_f rises by $+0.11$ eV for the T site and by $+0.40$ eV for the I site. However, there are inconsistencies in the values for ΔE_f in the literature: It is reported as -2.38 in Gunji and Kamimura[22] (hereafter referred to as GK) and as -0.17 eV in Hayami[26] (hereafter referred to as HA), while we obtained $+0.30$ eV in the present calculations, which amounts to a considerable discrepancy of more than 2 eV.

The calculated formation energies are listed in Table I. Note that the listed values for ΔE_f are represented in units of per Li atom and these values are given differently in the original papers. Since the calculation methods and the parameters for the computation are different from calculation to calculation, it is not easy to trace the cause of this discrepancy. Even though all the calculations are based on the density-functional theory with pseudopotential scheme, the Gaussian basis functions are used in GK, whereas a 96-atom supercell is used in HA. For pseudopotentials of the Troullier-Matrins type, which are used in both HA and in our calculations, a cutoff energy of 30 Ry for plane-wave expansion is sufficient for achieving an energy resolution 10 meV per B atom.[17] This criterion has been already satisfied in both calculations. Needless to say, the k-point sampling affects the calculated value for the energy to a certain extent; however, the discrepancy is far greater than this uncertainty. Furthermore, the GGA is used in HA, and the difference in energy due to the GGA is less than 0.2 eV, as shown in Table I. In GK, the structural optimization was performed under restricted conditions, while full optimization over all atom positions and cell parameters was performed in our case. In addition, the criteria for the residual forces and stresses for the present calculations were more stringent than those used in other papers. In this sense, the present calculations can be considered to be more reliable. Nevertheless, by performing similar restricted optimization, we confirmed that the insufficiency in the structural optimization cannot be a major cause for the large discrepancy in the values of ΔE_f.

After scrutinizing the possible causes for this discrepancy, we eventually discovered that the most relevant cause was the way in which the reference state of the Li atom was chosen: The atomic state was chosen in GK and HA, while the solid state was used in the present calculations. The difference in ΔE_f between GK (or HA) and our calculations amounts to the cohesive energy $E_{\rm coh}$ of Li, which has been obtained as 1.63 eV in experiments.[40] Table I lists our results for ΔE_f with regards to both the solid state and the atomic state for Li. As shown in the table, when the atom state is taken as the reference for Li, the agreement between the calculations in GK and our own calculations becomes closer. The cohesive energy $E_{\rm coh}$ of Li is calculated within both the LDA and the GGA. Furthermore, the solid state Li has been used for metallic Li (bcc structure), with $10 \times 10 \times 10$ k-point sampling. There is a well-known disposition of the LDA to overestimate the cohesive energy of solids,[41] and it has been widely known that the GGA can correct this error in many cases. By considering the difference between calculations made with the LDA and the GGA, the error of the calculated formation energy is $\sim$0.2 eV. If only a

TABLE I. Pseudopotential calculations for the formation energy ΔE_f of Li for α-boron for various configurations: Li (O site), Li_2 ($T \times 2$), and Li_3 ($O + T \times 2$). The present calculations performed by using OSAKA2K (denoted as O2K) and QUANTUM ESPRESSO (QE) are compared to other calculations, namely, GK (Ref. 22) and HA (Ref. 26). The calculation conditions in the structural optimization are as follows: k-point $n_{\rm kpt}$, plane-wave cutoff energy $E_{\rm cut}$ in Ry, tolerance of force Δf in Ry/Bohr, and stress $\Delta\sigma$ in Ry/Bohr^3. The cohesive energy $\Delta E_{\rm coh}$ of Li is also listed in the last rows.

					ΔE_f eV/(Li atom)			
	Conditions				Li		Li_2	Li_3
Code	$n_{\rm kpt}$	$E_{\rm cut}$	Δf	$\Delta\sigma$	LDA	GGA	LDA	LDA
Reference Li: Solid								
O2K	2^3	70	$<10^{-3}$	$<10^{-6}$	+0.52	+0.54		
QE	10^3	70	$<10^{-5}$	$<10^{-6}$	+0.30	+0.49	+1.72	+0.68
Reference Li: Atom								
O2K					−1.45	−1.28		
QE					−1.74	−1.42	−0.33	−1.37
GK (Ref. 22)			$10^{-1} - 10^{-3}$		−2.38		−1.15	−1.54
HA (Ref. 26)					−0.41			
$\Delta E_{\rm coh}$ of Li	(eV/atom)		LDA	GGA				
O2K			1.97	1.82				
QE			2.07	1.91				
Expt. (Ref. 40)			1.63					

comparison of the formation energies in a systematic variation is of interest, further accuracy is expected.

It is meaningless to discuss which way is correct to choose the reference state, except in cases when the reaction under consideration is explicitly specified. In experiments, various states can be chosen as the starting condition (e.g., starting materials and T). Then, all the energies in Eq. (1) should be replaced with the corresponding free energies or chemical potentials μ(B). In handbooks containing thermodynamic data, the enthalpy of formation ΔH_0 is customarily defined by referring to the most stable state of a material at standard temperature and pressure. For Li, the natural reference state is a metallic state with a bcc structure. For solids, the temperature dependence of the chemical potential is known to be not strong, and the present result indicating a positive ΔE_f would not change unless extreme conditions are imposed. As long as the metallic Li is used as the starting material, we can therefore conclude that the doping into α-boron is difficult. On the other hand, when gaseous Li is used, the temperature dependence of the chemical potential cannot be ignored. This issue is discussed below.

B. Structural changes

In this section, the effects of Li doping in α-boron are investigated. Hereinafter, Li is assumed to be located at the most stable site, i.e., the O site.

a. Structural changes. A comparison of the structural parameters for nondoped and doped boron is summarized in Table II. In the calculations presented in GK, the cell angle $\alpha_{\rm rh}$ is fixed, and hence the structural anisotropy should not be changed. However, the change in anisotropy, although small, has important significance, as seen later. As shown for the case of nondoped α-boron, the GGA yields results that are in closer agreement with the experiment than those obtained with the LDA. For the structural changes, a trend showing that a_0 increases (by +1.9% in our case) and $\alpha_{\rm rh}$ decreases by −1.2% on doping is clearly seen. This indicates that an elongation of the unit cell along the c axis occurs, accompanied with Li insertion.

Considering the change in the bond lengths, we obtained more detailed information about the structural deformation. Inside the icosahedron, there are four independent intraicosahedral B-B bonds shown in Fig. 1. Upon doping, p-p and p-e bonds become elongated, whereas e-e^* and p-e^* bonds, which are almost in the ab plane, become contracted. This implies an elongation of the icosahedron along the c axis. In this regard, the intericosahedral bond r_2 shows considerable elongation. All these changes in bond length are consistent well with respect to the elongation of the cell along the c axis. On average, the bond lengths are elongated by 0.78%, which indicates that the bonding of α-boron is weakened by Li doping. It should be noted that the intericosahedral three-center bond r_3 does not change. This suggests that the relative strength of the three-center bond increases as compared to the other bonds. This explains why the change in the angle $\Delta\alpha_{\rm rh}$ is negative.

The above implication that the bonds are weakened upon doping is supported by the change in bulk modulus B (a decrease of 4.4% in our calculations), as well as by the phonon softening, which is discussed below. Indeed, softening is what is expected in ordinary semiconductors. For heavily doped diamond, softening is reported.[46,47] For semiconductors the valence and conduction bands are most clearly separated by bonding and antibonding characters, respectively. The introduction of any types of carriers, whether electrons or holes, causes weakening of the bonds either through occupying the conduction band or through the depleting valence band.[48] Therefore, it is indeed unusual to find a significant increase of about 80% for B in GK. One reason for this difference might be

TABLE II. Structural parameters of nondoped and Li-doped (at the O-site) α-boron. Lattice parameters a_0, α_{rh}, volume of unit cell V, bulk modulus B, and bond lengths. The listed bonds are shown in Fig. 1. For each quantity, the relative change with respect to the case of non-doped boron is shown in %.

	Cell parameters				Bond length (Å)						
	a_0	α_{rh}	V	B	Intra-					Inter-	
	(Å)	(deg)	(Å^3)	(GPa)	p-p	p-e^*	p-e	e-e^*	mean	r_2	r_3
	Nondoped										
Calculated											
Present	4.994	58.08	84.19	248	1.727	1.773	1.781	1.763	1.764	1.657	1.979
GK (Ref. 22)	5.063			233	1.74	1.80	1.79	1.78	1.781	1.67	2.02
HA (Ref. 26)	5.04	58.10	86.58								
VA (Ref. 38)	4.98	58.2	83.7		1.72	1.77	1.78	1.76	1.76	1.65	1.98
Experiment											
Ref. 42	5.057	58.06	87.40	200 (Ref. 43)	1.751	1.801	1.782	1.806	1.786	1.670	2.03
Ref. 44	5.0561	58.14	87.75		1.753	1.800	1.807	1.784	1.790	1.671	2.014
Ref. 45	5.091	57.84	88.68		1.765	1.816	1.820	1.786	1.801	1.641	2.017
	Li doped										
Present	5.089	57.34	237	87.48	1.739	1.755	1.847	1.747	1.787	1.692	1.979
(%)	+1.9	−1.2	+3.9	−4.4	+0.73	−1.02	+3.6	−0.91	+0.78	+2.1	0.0
GK (Ref. 22)	5.077			417							
(%)	+0.28			+79							
HA (Ref. 26)	5.20	57.7	94.17								
(%)	+3.2	−0.69	+8.8								

the insufficiency of their optimizing conditions. Nevertheless, the discrepancy is beyond what is expected to occur as a result of this insufficiency.

The present calculations suggest a useful approach to identifying Li incorporation in experiments: The characteristic changes are +1.9% in Δa_0 and −1.2% in $\Delta\alpha_{rh}$ per Li atom in an α-boron cell. These changes are easily determined by x-ray diffraction. For sparsely dissolved systems, this can provide a satisfactory estimate for the concentration of Li by assuming the Vegard law.

b. Charge density. All of the above changes in the bond lengths should be confirmed by examining the electronic charge density. Figure 2 shows the differences in charge density $\Delta\rho(\mathbf{r})$ before and after doping.

For all the bonds which show expansion, the charge density has decreased as seen in the intericosahedral two-center bond r_2 and the intraicosahedral p-e bond. On the other hand, the charge density has increased in the intericosahedral three-center bond r_3. This is consistent with the near absence of changes in the bond length r_3.

This figure also indicates how the orbital of the added electron provided from Li is distributed over the crystal. Around the Li atom, the charge density has increased in comparison with the case of nondoped α-boron. However, a more important increase is found at the intericosahedral three-center bond. The bonding nature of the bottom of the conduction band has been studied in a previous paper,[9] where it was found that the band has a bonding character in the intericosahedral three-center bond and an antibonding character in the intraicosahedral p-e bond. The increase in charge density at the three-center bond is a direct consequence of the fact that the extra electron added by doping fills the bottom of the conduction band. This induces shrinking of the unit cell in the ab-plane. This response of the three-center bond can be clearly seen when a H atom is inserted at the T site.[49] Therefore, the changes in the structure must provide reliable criteria about whether Li is incorporated into the desired O site.

c. Phonon properties. The changes in the phonon frequencies associated with the doping are presented in Table III. All of the phonon frequencies decrease on doping. At this point, the occurrence of softening due to doping is indisputable. Such softening is expected for typical semiconductors, as mentioned

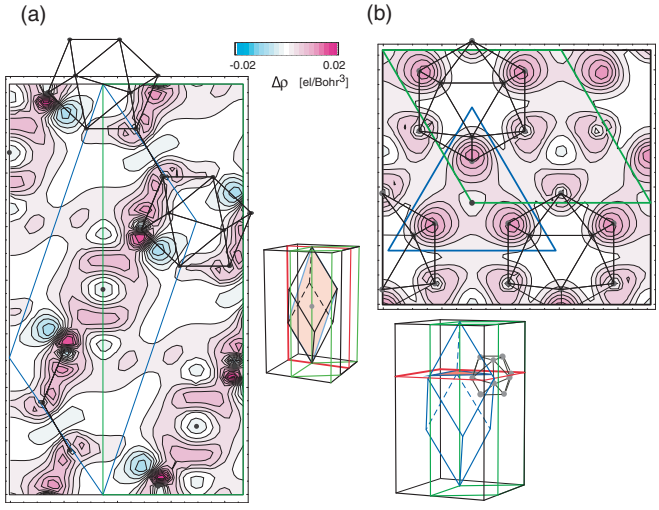

FIG. 2. (Color online) Differences in charge density $\Delta\rho(\mathbf{r})$ before and after doping. Red (blue) regions indicate an increase (decrease) in $\Delta\rho(\mathbf{r})$ (a) in the vertical plane, (b) in the ab plane including three e sites forming the three-center bond.

TABLE III. Calculated Raman frequencies (cm^{-1}) in nondoped and Li-doped α-boron. The relative change is shown in %.

Sym.	E_g	E_g	A_{1g}	E_g	E_g	A_{1g}	E_g	A_{1g}	E_g	A_{1g}
Nondoped										
Present	523	610	711	733	792	820	895	952	1141	1196
VA (Ref. 38)	529	608	708	729	790	815	890	947	1138	1192
Expt. (Ref. 50)	524	587	693	710	776	796	872	931	1125	1185
Li doped										
Present	284	505	590	643	651	778	848	884	1044	1114
(%)	−45.7	−17.2	−17.0	−12.3	−17.8	−5.1	−5.3	−7.1	−8.5	−6.9

above. Decrease in frequency of this order of magnitude can be easily observed by Raman spectroscopy.

A strong softening is found for the lowest E_g mode, where the frequency shift reaches almost half of the original one. This mode is known as the so-called ghost peak due to its exceptionally narrow Raman linewidth and other unusual properties.[50,51] Now, it has been discovered that the nature of this ghost peak is due to a librational mode, that is, rigid rotation of an icosahedron.[38] This mode is special in a sense that the frequency is primarily determined by angle forces.[52] The relevant angle forces are those associated with the intericosahedral bonds r_2. Accordingly, the softening of the librational mode suggests weakening of the angle forces of the intericosahedral bonding. This is in accordance with a widely accepted understanding that the intericosahedral bond r_2 is well described as a usual covalent bond. The covalent bond has a highly oriented character, a part of which is lost by spreading extra electrons.

Weakening of the angle force can be checked by investigating the charge distribution about the bond angle. Figure 3 shows a change in the charge distribution of the intericosahedral bond r_2. An angle restoring force is exerted when angle 1-2-6′ is changed. The strength of the exerted force is determined by the dependence of the adiabatic potential on the angle 1-2-6′. This dependence is reflected in the way of the charge distribution over the azimuthial angle ϕ, which is shown in the figure. The dependence of the charge density on the angle reflects the dependence of the adiabatic potential on the angle. As shown in Fig. 3(c), the dependence of the charge density on the angle is weakened by the doping. Hence, a softening of the librational mode is reasonably expected.

Considering the narrow linewidth of this librational mode, we can say more about the effect of doping on this mode. Shirai *et al.* disclosed that the most important factor in determining the linewidth $\Delta\omega$ is the two-phonon density of states $\rho_2(\omega)$ and, more specifically to α-boron, the difference part of $\rho_2(\omega)$.[52] For α-boron, the librational mode lies at the minimum in $\rho_2(\omega)$. The large softening of the frequency means a movement of the decay channels to lower a frequency region, where $\rho_2(\omega)$ significantly increases. Consequently, the extremely narrow linewidth is broadened considerably, which indicates that the "ghost" peak is changed to an ordinary peak.

The above-mentioned prominent changes in the librational mode can be regarded as more stringent criteria than the x-ray diffraction method for determining whether a Li atom occupies a desired position. The changes in the lattice parameter are not as sensitive to the specific site since they depend primarily on the average concentration.

C. β-boron

Let us move on to the case of Li doped β-boron. In this case there are experimental data for comparison.[29] On this basis,

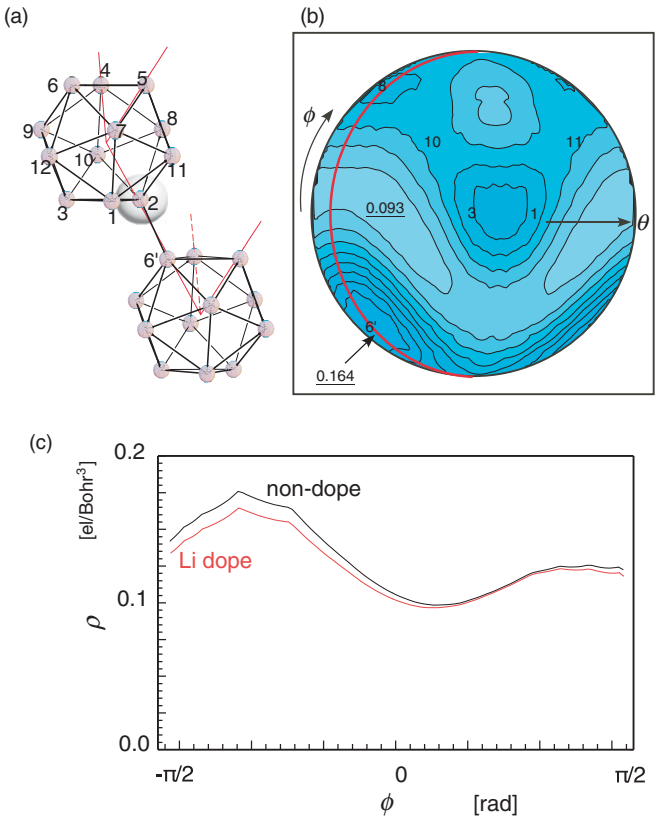

FIG. 3. (Color online) Distribution of the charge density around a p site in α-boron. (a) Around a p site (atom 2), a sphere is cut as indicated by the semitransparent sphere. The radius is 1/3 of the bond length of an intericosahedral bond 2-6′. (b) Charge distribution mapped onto the sphere around atom 2. A spherical coordinate system (θ,ϕ) is used. The neighboring atoms are projected onto the sphere and indicated by numbers. Underlined numbers indicate the maximum and the minimum of the charge density in el/Bohr^3. The unit step of the contours is 8 $me l/\text{Bohr}^3$. Along the red (gray) line, a line profile of the charge density is plotted in (c) for doped and nondoped α-boron.

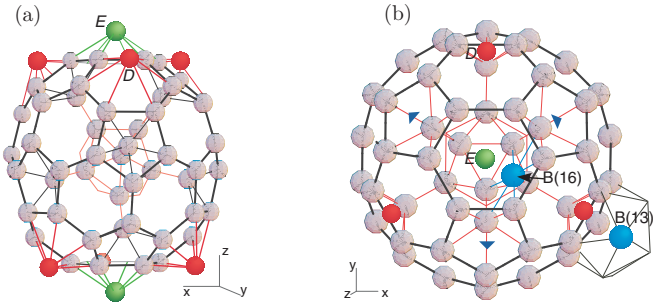

FIG. 4. (Color online) Interstitial D (red/light gray) and E (green/dark gray) sites of β-boron which are occupied by Li atoms. For clarity, these interstitial sites are shown as being attached to a B_{84} unit. It should be noted that these interstitial sites have other neighboring atoms which are not shown here. (a) Side view. The E site is on the main diagonal of the rhombohedral unit cell. Both the E and the D site are located above a hexagonal face of a B_{84} unit. (b) Top view. The faces of a B_{84} unit connected to a neighboring B_{84} units are indicated with blue triangles. Also shown with blue (gray) spheres are the interstitial site B(16) and the partially occupied cite B(13).

we are able to answer why Li incorporation is successful for β-boron and why it does not lead to the expected effects of carrier doping.

The crystal structure of β-boron is highly complex. Conventionally, the structure is denoted as B_{105}, where formally there are 15 irreducible sites labeled from B(1) to B(15). However, there are additional cites, labeled from B(16) to B(20), which are only partially occupied.[53–55] A structural refinement shows that the unit cell contains 106.7 atoms.[55] It is well known that there are numerous interstitial sites which accommodate a variety of guest atoms.[56] Some exhibit only partial occupancy, while others exhibit perfect occupancy. According to Kobayashi *et al.*,[29] the Li case corresponds to a case of perfect occupancy. There are two E sites and six D sites, resulting in a total of eight sites. The atomic arrangement around those sites are illustrated in Fig. 4. Both types are located above a hexagonal face of a B_{84} unit, with the additional feature that E sites are located on the principal axis. Note that D sites are slightly deflected from the center of the respective hexagon. A later refinement shows a more complicated configuration.[57]

Recent theoretical studies have clarified that the existence of defects is an intrinsic property of β-boron in a sense that these defects are properties of the ground state and are not caused by entropic contribution at high temperatures.[17–20] Ogitsu *et al.* have set forth the idea that the electronic structure of β-boron can be characterized as a frustrated system.[20] This is a common feature of boron-rich solids. In this way, the occupancy problem of β-boron is too complicated to manage in electronic calculations. Currently, the best we can do is use of perfect B_{105} as the matrix. Then, we fill all the E and D sites with eight Li atoms, and guess the effect of disorder.

The structural parameters as obtained through calculation and experiment are compared in Table IV. Close agreement with experiment is obtained for Li-doped β-boron (hereinafter denoted as Li_8B_{105}), as well as for nondoped β-boron. Upon doping, the cell of β-boron is expanded. In this case, the cell angle α_{rh} increases. This contrasts with the case of α-boron. As discussed in Sec. III B, the decrease in α_{rh} implies the strengthening of the intericosahedral three-center bond. However, for β-boron, there is no clear distinction between inter- and intraicosahedral bonds.

Once quantitative comparison is needed on the effects of Li doping on the structural parameters between different structures such as α- and β-boron, care must be taken as to evaluate the change of properties on the same ground. The changes of the lattice parameters must be evaluated by normalizing with respect to the concentration n of Li. The normalized changes are compared in Table IV. Although $\Delta(\ln a_h)/n$ is similar for α- and β-boron, $\Delta(\ln c_h)/n$ is larger for α-boron than for β-boron. This reflects the fact that the three-center bond for α-boron is strengthened by doping. These calculated changes can provide a conventional measure for the concentration of Li since the lattice parameters can be routinely obtained with sufficient accuracy.

The formation energy of Li for β-boron is obtained as -2.05 eV/Li atom. The negative sign of ΔE_f shows that forming a compound is easy. In this case, Li_8B_{105} is a stable compound with respect to the constituents, and this is consistent with experiment. In the spirit of Eq. (2), $+0.145$ eV/atom might be a more appropriate expression for the formation energy in the context of alloy physics. The above energetics shows the different status of Li doped in boron depending on the matrix, namely, an impurity for α-boron and a constituent of a compound for β-boron. Now, we discuss the reason why they are different. In Table V, the neighboring atoms around a Li atom are compared for α- and β-boron. By inspecting in this way, the local environments of the Li atoms do not appear to be strikingly different between these two crystals. The bond lengths are similar ($\sim$2.2 Å), and the numbers of coordination are also similar. However, the difference will be clarified by examining the electronic charge distribution. Figures 5 and 6 show the charge distribution over all the angles around the doped Li atom in α- and β-boron. The mapped sphere is taken with a radius of half of the bond to the nearest neighbor.

For α-boron, the charge is distributed relatively homogeneously in all directions, in contrast to β-boron. The charge density fluctuates in a relatively narrow range between 0.012 and 0.040 $mel/Bohr^3$. On the other hand, in both E and D sites of β-boron, the charge distribution shows stronger dependence on the angle. For an E site, it is concentrated at a specific latitude, and for a D site, it is more concentrated in the directions of atoms 28 and 31, the width of the charge density between the maximum and the minimum being larger as compared with the case of α-boron. In fact, the bond 28–31 is contracted by 0.5% on doping, indicating strengthening of the bond. These observations show that the Li atoms in β-boron exhibit more covalent character, which lowers the local energy around the defect. This is why Li atoms can be easily accommodated into β-boron and strengthen the neighboring B-B bonds.

Readers might notice the large errors in the bond lengths in Table V. We believe that these errors are due to the inappropriate way of treating defects in our cell size, namely, there is no randomness in our calculations on the primitive cell. Interstitial site B(16) is close to one of the D or E sites

TABLE IV. Calculated structural parameters of Li@β-B (Li_8B_{105}). a_h (Å), c_h (Å), and V are lattice constants and the volume of hexagonal cell, respectively. $\frac{\Delta \ln a}{n}$, $\frac{\Delta \ln c}{n}$, and $\frac{\Delta \ln a}{n}$ are the relative change of lattice constants with respect to the concentration n of Li in atom %. ΔE_f represents the formation energy per Li atom in eV/(Li atom).

	a_0 (Å)	α_{rh} (deg)	a_h (Å)	c_h (Å)	V (Å^3)	$\frac{1}{n}\frac{\Delta a_h}{a_h}$ [$\times 10^{-2}$ %/(atom %)]	$\frac{1}{n}\frac{\Delta c_h}{c_h}$	$\frac{1}{n}\frac{\Delta V}{V}$	ΔE_f [eV/(Li atom)]
Li@β-B									−2.05
				Nondoped					
Present	10.041	65.30	10.835	23.562	239.6				
Expt. (Ref. 53)	10.139	65.2	10.9252	23.8142	246.2				
Error (%)	−0.96	+0.15	−0.83	−1.1	−2.7				
				Li-doped					
Present	10.084	65.49	10.908	23.625	243.4				
Expt. (Ref. 29)	10.2149	64.92	10.9654	24.0495	250.4	5.2	14.0	24.1	
Error (%)	−1.2	+0.9	−0.5	−2.0	−2.8				
Change (%)	+0.43	+0.29	+0.67	+0.27	+1.6	9.5	3.8	22.6	
Li@α-B									+0.30
Change (%)	+1.9	−1.2	+0.72	+2.4	+3.9	9.4	31.8	50.4	

(see Fig. 4). In addition, some B(13) sites display vacancies. Our experience on studying β-boron is that variations of this order of magnitude are found in the bond lengths around defects.[17] It is reasonable to assume that the presence of such defects modifies the bond length and alters its perfect structure. However, it is not as obvious whether vacancies (or interstitial defects) cause contraction (or expansion) of the neighboring bonds, as indicated in studies on vacancies in silicon.[58,59]

D. Electronic characters

The prominent contrast between α- and β-boron under the effect of Li doping must be reflected in their electronic structures. In this section, we describe the differences in the electronic structures, which are of crucial importance for the valence control.

Figure 7 shows the changes in the band structure of α-boron induced by Li doping. As seen in the figure, the effect of Li doping produces just an almost rigid-band shift of the original band structure. This point was first mentioned by GK,[22] and it has been confirmed in the present paper. Although rigid-band shifts are often referred to in the literature, it is indeed rare to be observed in actual materials with heavy doping (as high as 7 atom %). Only few are known to exhibit a rigid-band shift, such as K_3C_{60} (Ref. 60) and Li-doped carbon clathrate.[61]

In Fig. 8, the effects of Li doping on the electronic structure are compared for α- and β-boron. The density of states (DOS) spectra were obtained by using a $6 \times 6 \times 6$ k grid, where $E_{cut} = 70$ Ry for α-boron and 45 Ry for β-boron. For α-boron, as shown in the figure, Li doping does not affect the main features of the electronic structure of the host crystal, resulting in a rigid-band shift. More precisely, however, there is an important effect manifested in a shrinking of the energy gap by 0.35 eV. This is caused by the lowering of the bottom of the conduction band due to electrons occupying the three-center bonds. As described in Sec. III B, additional electrons enter the three-center bond, which is a part of the bottom of the conduction band.[9] Due to the bonding nature of this part, the energy is lowered. Aside from this shrinking of the energy gap, the effect of Li doping is simply manifested in a rigid-band shift. In partial DOS, Li components diminish toward the top of the valence band. From a slightly different point of view, we can interpret this as a result of a bonding requirement that is satisfied to such an extent in α-boron,[21] as in tetrahedrally

TABLE V. The neighboring atoms around a Li atom in α-boron (denoted as LiB_{12}) and β-boron (Li_8B_{105}). The bond lengths are shown in Å. The experimental data are taken from Ref. 29. For LiB_{12}, the bond length is indicated by multiplying the relevant value by the number of bonds. For Li_8B_{105}, in entry "bond," the numbers should be read as the atom index of the bond (the index of irreducible sites) × the number of bonds. The atom indices are the same as those in Fig. 6. The indices of irreducible sites are in accordance with Ref. 29.

	LiB_{12}	Li_8B_{105}							
	O site	E site				D site			
Neighbor	Calculated	Bond	Calc.	Exp.	Error	Bond	Calc.	Exp.	Error
First	2.172 × 6	36(1) × 6	2.253	2.11	6.7	28(1) × 2	2.129	2.28	−6.6
Second	2.587 × 12	73(9) × 3	2.428	2.44	−0.5	38(2) × 2	2.274	2.27	0.1
Further		75(10) × 3	2.578	2.80	−7.9	101(13) × 1	2.349	2.25	4.4
Distant		85(11) × 3	2.575	2.84	−9.3	40(2) × 1	2.355	2.51	−6.2
						91(12) × 1	2.419	2.10	15.2
						49(3) × 2	2.425	2.29	5.9

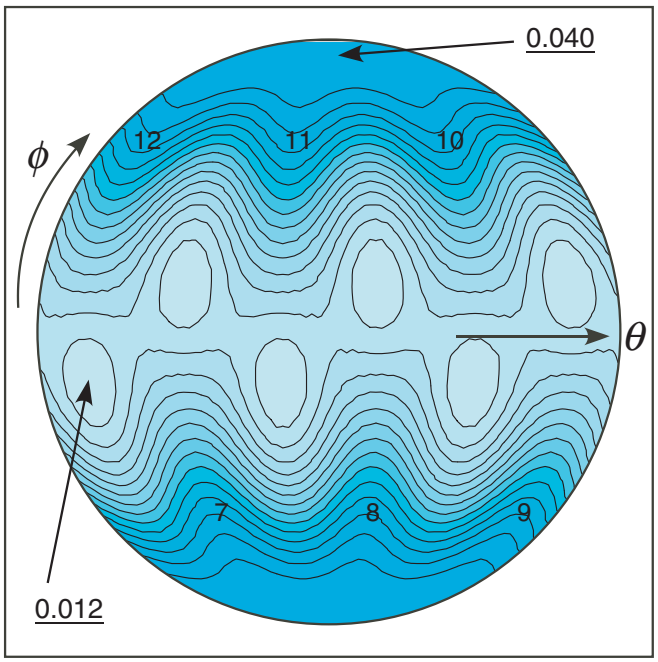

FIG. 5. (Color online) Spherical map of the charge density around Li at the O cite in α-boron. The sphere is taken with a radius of half of the bond to the nearest neighbor. The notations are the same as in Fig. 3. The atom labels are shown there, and the unit step of the contours is 2 mel/Bohr^3.

coordinated semiconductors, that there is no choice for extra electrons other than to enter the conduction band. In early studies of the electronic structure of boron crystals, it was argued, in analogy with molecular orbitals of B_{12} molecules, that weak three-center bonds participate in the top of the valence band, and therefore the replacement of these bonds with strong covalent bonds is the driving force of the formation of complex structures such as β-boron. However, this analogy is not pertinent[21] since in reality the valence band of α-boron is not sufficiently similar to that of a single B_{12} molecule. The intericosahedral bonding is so strong that the valence bands have been reconstructed, leaving the three-center bond out of the valence band. This completes the valence bands with a fully bonding character. However, the three-center bonds play a role when they become shortened, as demonstrated in high-pressure experiments.[9]

On the other hand, the effect of Li doping on β-boron is completely different. For β-boron, it induces not only a shrinking of the energy gap, but also alterations in the structure of the valence band. It should first be noted that even for nondoped crystals the calculations do show that the Fermi level lies 0.5 eV below the top of the valence band, which results from our assumption of a perfect B_{105} structure. Standard band theory tells us that an odd number of electrons necessarily lead to metallic properties. However, in experiments, β-boron behaves as a semiconductor. This disparity is a long-debated issue in boron physics, and as yet it is not satisfactorily resolved.[16,20,21] At present, we can only say that the defects observed experimentally are essential for the gap problem. Calculations show that the energy gap is sensitive to the presence of defects,[7] even though only B(16) are taken into account in the calculation. Since this issue is too broad to discuss here, we simply assume that the valence band is fully occupied for some unknown reason, and we concentrate on the relative changes in the electronic structure instead.

As seen in Fig. 8, the top of the valence band of β-boron is significantly altered on doping. At approximately 8 eV, we can see an almost isolated peak which resembles a gap state. It is clear that the top of the valence band has been reconstructed by Li doping. We can consider that similar band alterations would occur for nondoped β-boron, namely, that partially occupied sites interact with the top of the valence band in order to fulfill the bonding requirements of that band, which renders the crystal an insulator. In effect, localized states will be singled out from the valence band. By the nature of band calculation in periodic systems, we cannot claim unambiguously whether the present state is indeed a localized state, unless extremely large supercells are used. However, it is highly likely that this is the case. A recent proposal for characterization of β-boron as a frustrated system is highly convincing in this respect[20] since the frustration of the valence band welcomes partially occupied defects.

The idea that the invincibility of defect states is inherent in icosahedron-based boron-rich solids has also been proposed for boron carbides.[62] Accordingly, even though extensive efforts have been made to dope β-boron,[14,15,30] as yet metallization has not been achieved, to the best of our knowledge. In this respect, metallization of α-boron is desirable, in spite of the difficulties associated with the preparation of the host crystal.

IV. EFFICIENT DOPING METHOD

Up to this point, it has been revealed that, under normal conditions, Li-doped α-boron is classified as an impurity system, similarly to typical doped semiconductors. However, the formation energy is small ($\sim$0.5 eV). For Si, ΔE_f is of the order of several eV for typical dopants.[63,64] For heavily B-doped diamond or B-doped silicon, for which metallization has been achieved, ΔE_f is less than 1 eV.[65] Hence, it is not at all impossible to achieve heavy doping for α-boron by some means. In the last section, an efficient method for doping α-boron is discussed on the basis of thermodynamic considerations.

Let us first evaluate the concentration of Li in α-boron. In the following discussion, the formation energy defined in Eq. (1) will be replaced by the enthalpy of formation ΔH_f by adding the pV term, if appropriate. As mentioned above, the enthalpy of formation ΔH_f is not a material constant but varies depending on the starting state of the reaction. The present results of $+0.5$ eV for the solid state and -1.3 eV for the gaseous state give the limiting values for ΔH_f. In this regard, the gaseous state is desirable for the starting state of Li. Soga *et al.* achieved Li-doped α-boron by using vapor diffusion processing.[30] However, only a small fraction of sample contains Li impurity, and the Li concentration has not been well characterized. At finite temperatures, the chemical potential of gaseous Li $\mu^{(g)}$(Li) decreases and ΔH_f increases toward positive values. An example of dependence of ΔH_f on temperature is seen for hydrogen doping of α-boron.[49] In studying impurities in semiconductors, it is a common practice

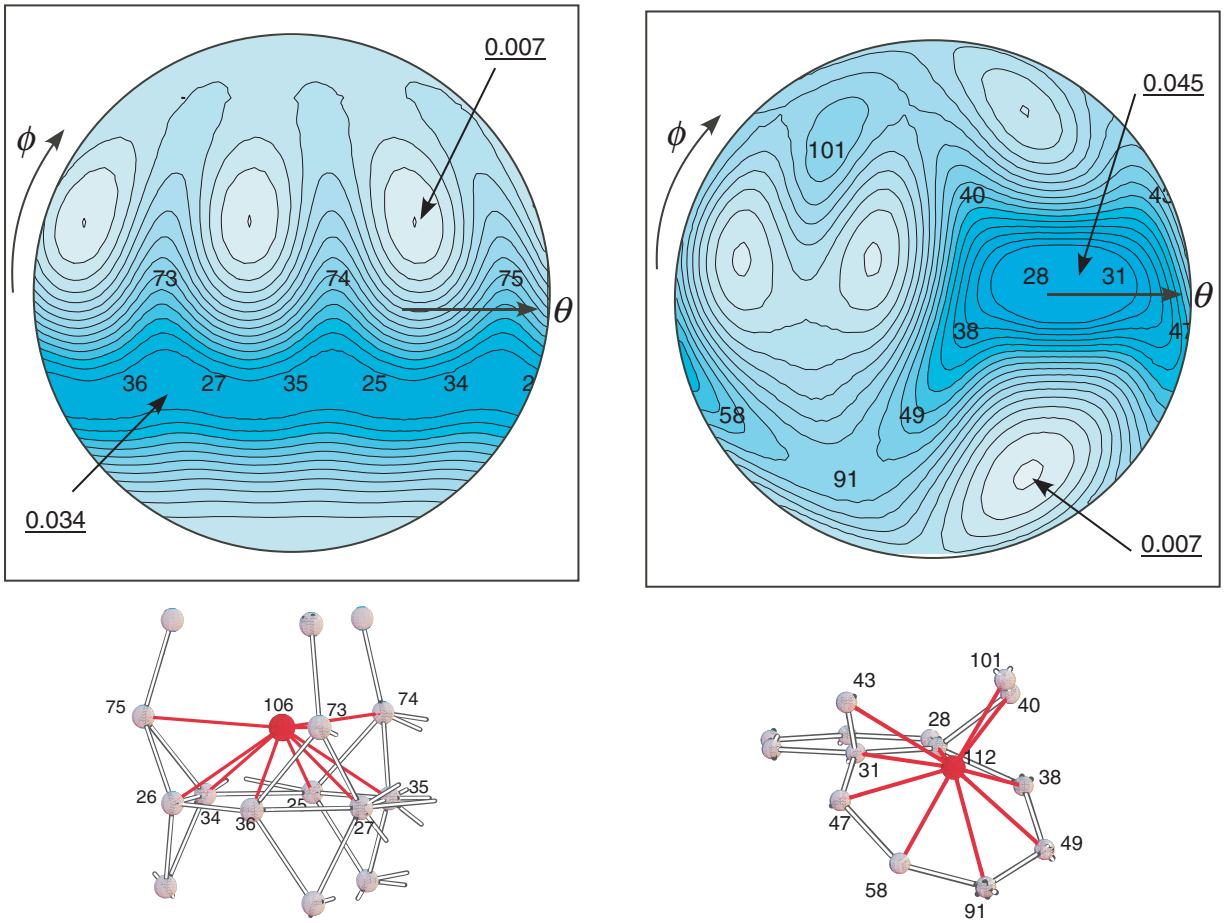

FIG. 6. (Color online) Spherical map of the charge density around Li in β-boron: (Left-hand side) Li atom in an E site at 106, (right-hand side) a D site at 112. The configuration of the neighboring atoms is shown below, where the notations are the same as in Fig. 3. The unit step of the contours is the same as in Fig. 5.

to calculate the concentration of impurities as a function of the chemical potential of the source materials.

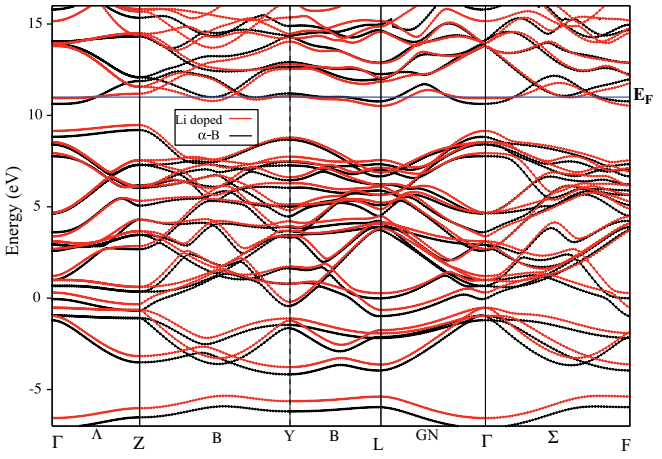

FIG. 7. (Color online) Changes in the electronic energy band of α-boron with Li doping. The red (gray) curves indicate the band of Li-doped α-boron, while the black curves correspond to that of nondoped α-boron. For the notation of symmetry points and lines, please see Ref. 9.

Figure 9 shows an example where the concentration of Li is calculated as $N_0 \exp(-\Delta H_f/kT)$, where N_0 is the density of the available sites. The temperature T is chosen as 1300 K, which is almost the upper bound for the stability of α-boron.[66,67] The worst case occurs when solid Li is chosen for the reference. In this case, the dependence of $\mu^{(s)}$(Li) on the temperature can be ignored, and hence the value 0.5 eV at $T = 0$ K can be used over the entire range of T. Then, the concentration of Li is only 0.01 atom %. Although this is a substantial amount according to semiconductor standards, it may be too small for the purpose of metallization. In our experience with B-doped diamond, concentrations as high as 1 atom % are desirable.

Our proposal for solving this difficulty involves the use of high pressure. We have devised this idea by considering the large difference between the respective bulk modules for Li and B. Under pressure, the enthalpy of formation is strongly dependent on the volume.

Figure 10 shows the dependence of ΔH_f of Li on the pressure for α-boron when solid Li is taken as the reference. The effects of temperature are not included. We can see a decrease in ΔH_f as the pressure increases. The sign of ΔH_f becomes negative at 3 GPa. This shows the possibility for forming the compound LiB_{12} at high pressure. This decrease

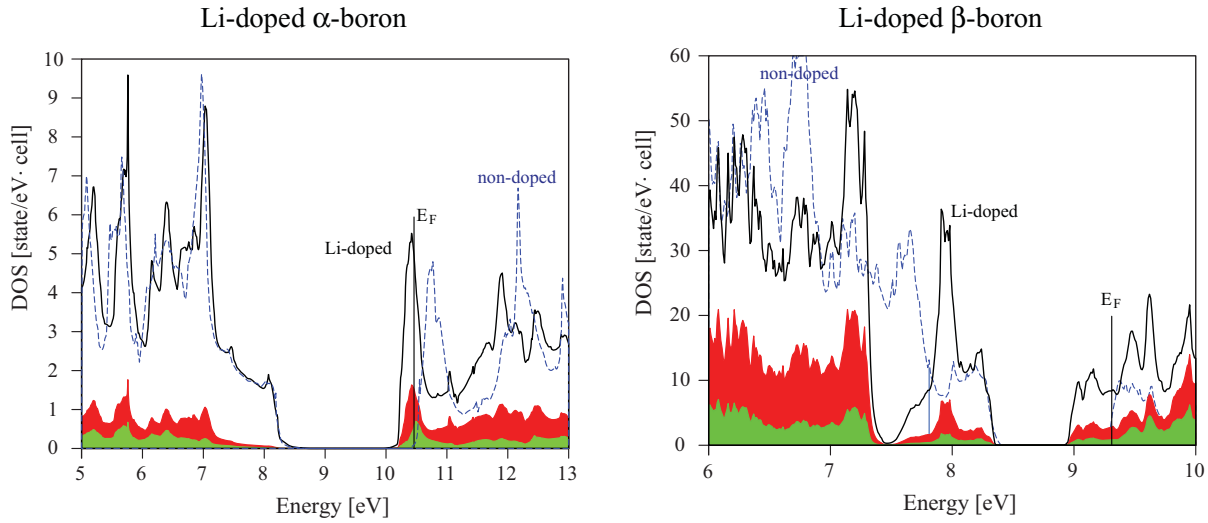

FIG. 8. (Color online) DOS spectra of Li-doped α- and β-boron (black solid lines) compared with those of the respective nondoped host crystals (blue dashed lines). The origin for the energy has been aligned with the top of the valence band between nondoped and doped crystals. Contributions of the atomic orbitals of Li (green/gray: s; red/dark gray: p orbital) are superimposed with a magnification level of 10.

in ΔH_f is easily understood by considering the following argument. The dependence of the enthalpy $\Delta H(p)$ on pressure can be expanded to the second order in p as

$$\Delta H(p) = \Delta H^0 + bp + \tfrac{1}{2}ap^2, \tag{3}$$

where the coefficients are given as $b = \Delta V_0$ and $a = -\Delta(V_0/B_0)$. The subscript 0 denotes those quantities that are evaluated at $p = 0$. On the assumption that the linear term is dominant, when b is negative, $\Delta H(p)$ decreases as p is increased, and vice versa. The coefficient b of the linear term is given as the difference of the free volume ΔV_0 before and after the reaction. As seen in Table VI, the free volume has decreased after the reaction (Li incorporation), and therefore a decrease in ΔH_f is expected. In this regard, the approximation Eq. (3) is plotted in Fig. 10. The linear relationship is valid only when p is smaller than the smallest value among the B_0 of all components. In other words, we can state that the softest material controls the dependence on pressure.

The decrease in free volume is reasonable. It is easier for the denser (and thereby stiffer) material to incorporate the less dense (and thereby softer) material inside its structure at high pressure than vice versa. From this observation, we can deduce the simple rule that *softer materials can be easily doped to stiffer materials under high pressure*.[7]

Regardless of the simplicity of this rule its applicability is rather wide. The rule is based upon a well-known principle of thermodynamics, namely, *Le Chatelier's principle*, which states that, for a system at equilibrium, a perturbation induces a process that attenuates the initial perturbation. In the present case, the perturbation is a change in volume. In fact, the inclusion of atoms of gases, such as He, into a specimen at high pressure is a daily experience for researchers experimenting with high pressures. An affirmative example can be given with

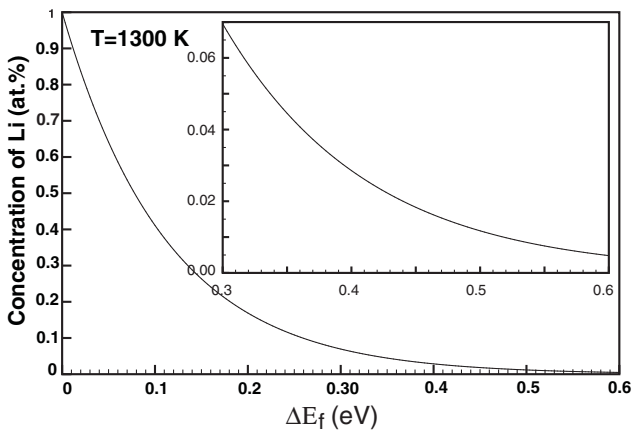

FIG. 9. The concentration of Li in α-boron as calculated from the formation energy ΔE_f. The inset shows an expanded form in order to resolve the Li concentration at approximately $\Delta E_f = 0.3$–0.6 eV.

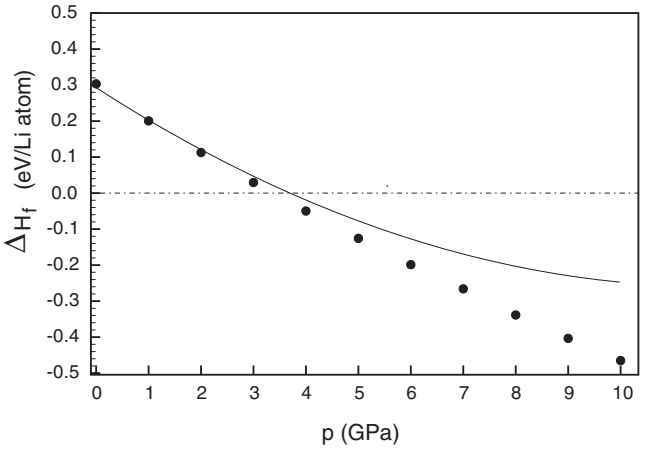

FIG. 10. Pressure dependence of the enthalpy of formation ΔH_f of Li in α-boron. The sign of ΔH_f becomes negative when the external pressure reaches nearly 3 GPa in LiB_{12}. The solid line corresponds to an approximate form of Eq. (3).

TABLE VI. Pressure dependence of the enthalpy of formation.

	V_0 (eV/GPa)	B_0 (GPa)	$-V_0/B_0$ (eV/GPa^2) $\times 10^{-3}$
Li@α-B	0.5412	221.2	−2.447
α-B	0.5216	225.5	−2.313
Li	0.1133	14.0	−8.091
Δ	−0.0937		7.958

doped clathrates. Yamanaka *et al.* have used high-pressure processing to synthesize Ba_8Si_{46}.[68] The reaction that they used is

$$8BaSi_2 + 30Si \rightarrow Ba_8Si_{46}. \quad (4)$$

They pointed out that the free volume of Ba_8Si_{46} is 15% smaller than that of the reactant mixture, from which they found it efficient to use high-pressure synthesis. In this regard, high-pressure doping methods are becoming increasingly popular. For example, heavily B-doped diamond has been synthesized at high pressure.[69] The reaction of this method has been studied theoretically, and higher concentrations of B are suggested for high pressure levels.[65] In zeolites, higher concentrations of K atoms have been obtained through high-pressure doping as compared with conventional methods.[70] Iron-based layered compounds, in which superconductivity has recently been discovered, are also synthesized by adopting high-pressure techniques, although the merits of the method are not fully understood.[71]

V. CONCLUSION

We have disclosed the striking differences in the effect of Li doping for apparently similar host crystals, namely, α- and β-boron. Li-doped α-boron can be characterized essentially as an impurity system, even for the stoichiometric compound LiB_{12}, because α-boron finds the perfect form in its own structure in a sense that the bonding requirement is most satisfactorily fulfilled in nondoped form. In effect, the doping causes weakening of the bonding characters, softening in the elastic properties, and a positive formation energy in α-boron. In contrast, Li-doped β-boron can be characterized as a stable compound, as indicated by experiment. This results from the idea that the electronic nature of β-boron is a frustrated system, and thus the inclusion of guest atoms is in accordance with its own bonding requirements. This leads to negative formation energy.

The present results for the structural and phonon properties provide useful criteria for detection of Li inclusion, which can be easily determined by conventional methods, such as x-ray diffraction or Raman spectroscopy. In particular, for α-boron, the present results predict prominent changes, that is, a decrease in the rhombohedral angle α_{rh} as well as considerable softening (and broadening) in the librational mode ω_l.

The difficulties associated with doping also have another side, namely, rigid-band shift, which is desirable for the electrical activity of doping. For β-boron, the ease of doping results in difficulties in electrical activity. The present value of $\Delta E_f = +0.5$ eV for α-boron is not as large for the formation energy of impurities in semiconductors, and it would be possible to achieve high concentration of Li by changing the initial conditions of the reaction. In this regard, we devised a rather efficient high-pressure doping method, in which the application of pressure higher than 3 GPa turns Li-doped α-boron into a stable compound. Such pressures are not difficult to achieve with the present capabilities of high-pressure synthesizing technology.

ACKNOWLEDGMENTS

We thank Kimura and Soga for occasional discussions on the aspects of experimentation in this study and on the complex defects of β-boron. This work was partly supported by a Grant-in-Aid for Scientific Research in Priority Areas "Areas of New Materials Science Using Regulated Nano Spaces" (No. 20045009) of MEXT, Japan. One of the authors (H.D.) received financial support from The Murata Science Foundation.

*Present address: Senior Research Fellow Center, Ehime University, 2–5 Bunkyo-cho, Matsuyama, Ehime 790-8577, Japan.
†koun@sanken.osaka-u.ac.jp

[1] M. I. Eremets, V. V. Struzhkin, H. Mao, and R. J. Hemley, Science **293**, 272 (2001).
[2] S. K. Bose, T. Kato, and O. Jepsen, Phys. Rev. B **72**, 184509 (2005).
[3] E. A. Ekimov, V. A. Sidorov, E. D. Bauer, N. Mel'nik, N. J. Curro, J. D. Thompson, and S. M. Stishov, Nature (London) **428**, 542 (2004).
[4] E. Bustarret *et al.*, Nature (London) **444**, 465 (2006).
[5] Y. Takano, M. Nagao, I. Sakaguchi, M. Tachiki, T. Hatano, K. Kobayashi, H. Umezawa, and H. Kawarada, Appl. Phys. Lett. **85**, 2851 (2004).
[6] Z. A. Ren, J. Kato, T. Muranaka, J. Akimitsu, M. Kriener, and Y. Maeno, J. Phys. Soc. Jpn. **76**, 103710 (2007).
[7] K. Shirai, H. Dekura, and A. Masago, J. Phys.: Conf. Ser. **176**, 012001 (2009).
[8] K. Shimizu, M. Kaneshige, Y. Hashimoto, T. Nagatochi, H. Hyodo, and K. Kimura, Physica C **470**, S631 (2010).
[9] K. Shirai, H. Dekura, and A. Yanase, J. Phys. Soc. Jpn. **78**, 084714 (2009).
[10] K. Shirai, H. Dekura, Y. Mori, Y. Fujii, H. Hyodo, and K. Kimura, J. Phys. Soc. Jpn. **80**, 084601 (2011).
[11] R. Schmechel and H. Werheit, J. Phys. Condens. Matter **11**, 6803 (1999).
[12] C. Wood and D. Emin, Phys. Rev. B **29**, 4582 (1984).
[13] D. Emin, in *The 10th International Symposium on Boron, Borides, and Related Compounds*, edited by D. Emin, A. C. Switendick, B. Morosin, C. L. Beckel, and T. Aselage, AIP Conf. Proc. No. 231 (AIP, New York, 1991), p. 65.
[14] H. Matsuda, T. Nakayama, K. Kimura, Y. Murakami, H. Suematsu, M. Kobayashi, and I. Higashi, Phys. Rev. B **52**, 6102 (1995).
[15] H. Hyodo, S. Araake, S. Hosoi, K. Soga, Y. Sato, M. Terauchi, and K. Kimura, Phys. Rev. B **77**, 024515 (2008).

[16]H. Werheit, J. Phys.: Conf. Ser. **176**, 012019 (2009).
[17]A. Masago, K. Shirai, and H. Katayama-Yoshida, Phys. Rev. B **73**, 104102 (2006).
[18]M. J. van Setten, M. A. Uijttewaal, G. A. de Wijs, and A. de Groot, J. Am. Chem. Soc. **129**, 2458 (2007).
[19]M. Widom and M. Mihalkovič, Phys. Rev. B **77**, 064113 (2008).
[20]T. Ogitsu, F. Gygi, J. Reed, Y. Motome, E. Sxhwegler, and G. Galli, J. Am. Chem. Soc. **131**, 1903 (2009).
[21]K. Shirai, J. Superhard Mater. **32**, 205 (2010); **32**, 332 (2010).
[22]S. Gunji, H. Kamimura and T. Nakayama, J. Phys. Soc. Jpn. **62**, 2408 (1993); S. Gunji and H. Kamimura, Phys. Rev. B **54**, 13665 (1996).
[23]H. Dekura, K. Shirai, and H. Katayama-Yoshida, J. Phys. Condens. Matter **19**, 365241 (2007); Physica B **401-402**, 702 (2007).
[24]Hydrogen is another candidate although its formation energy is not small. This concerning is described in another paper (Ref. 49).
[25]W. Hayami, Phys. Rev. B **60**, 1523 (1999).
[26]W. Hayami, T. Tanaka, and S. Otani, J. Phys. Chem. A **109**, 11975 (2005).
[27]W. Hayami and S. Otani, J. Phys. Chem. C **112**, 2711 (2009).
[28]Very recently, Li doping of α-boron has been succeeded by Kimura's group. They reported to observe a piece of superconductivity evidence: T. Nagatochi, H. Hyodo, K. Soga, Y. Sato, M. Terauch, and K. Kimura, Meeting Abstracts of PSJ, Vol. 64, Issue 1, Part 4 (2009), 30p-YG-3; T. Nagatochi, H. Hyodo, K. Soga, Y. Sato, M. Terauch, F. Esaka, and K. Kimura, Meeting Abstracts of PSJ, Vol. 65, Issue 1, Part 4 (2010), 22p-GR-13.
[29]M. Kobayashi, I. Higashi, H. Matsuda, and K. Kimura, J. Alloys Compd. **221**, 120 (1995).
[30]K. Soga, A. Oguri, S. Araake, M. Terauchi, A. Fujiwara, and K. Kimura, J. Solid State Chem. **177**, 498 (2004).
[31]C. Kittel and H. Kroemer, *Thermal Physics*, 2nd ed. (Freeman, New York, 1984).
[32][http://www.cmp.sanken.osaka-u.ac.jp/~koun/osaka.html].
[33]P. Giannozzi *et al.*, J. Phys. Condens. Matter **21**, 395502 (2009).
[34]J. P. Perdew and A. Zunger, Phys. Rev. B **23**, 5048 (1981).
[35]J. P. Perdew, K. Burke, and M. Ernzerhof, Phys. Rev. Lett. **77**, 3865 (1996).
[36]N. Troullier and J. L. Martins, Phys. Rev. B **43**, 1993 (1991).
[37]L. Kleinman and D. M. Bylander, Phys. Rev. Lett. **48**, 1425 (1982).
[38]N. Vast, S. Baroni, G. Zerah, J. M. Besson, A. Polian, M. Grimsditch, and J. C. Chervin, Phys. Rev. Lett. **78**, 693 (1997).
[39]S. Baroni, P. Giannozzi, and A. Testa, Phys. Rev. Lett. **58**, 1861 (1987).
[40]C. Kittel, *Introduction to Solid State Physics*, 6th ed. (Wiley, New York, 1986).
[41]S. Lee, D. M. Bylander, and L. Kleinman, Phys. Rev. B **42**, 1316 (1990).
[42]B. F. Decker and J. S. Kasper, Acta Crystallogr. **12**, 503 (1959).
[43]B. Morosin, A. W. Mullendore, D. Emin, and G. Slack, in *The International Conference on Boron-Rich Solids*, edited by D. Emin, C. L. Beckel, I. A. Howard, C. Wood, and T. Aselage, AIP Conf. Proc. No. 140 (AIP, New York, 1986), p. 70.
[44]G. Will and B. Kiefer, Z. Anorg. Allg. Chem. **627**, 2100 (2001).
[45]M. Fujimori, T. Nakata, T. Nakayama, E. Nishibori, K. Kimura, M. Takata, and M. Sakata, Phys. Rev. Lett. **82**, 4452 (1999).
[46]M. Hoesch, T. Fukuda, T. Takenouch, J. P. Sutter, S. Tsutsui, A. Q. R. Baron, M. Nagao, Y. Takeno, H. Kawarada, and J. Mizuki, Sci. Technol. Adv. Mater. **7**, S31 (2006).
[47]E. Bourgeois, E. Bustarret, P. Achatz, F. Omnès, and X. Blase, Phys. Rev. B **74**, 094509 (2006).
[48]We notice a few examples opposing this trend. For fullerides, introduction of alkali metals into C_{60} causes a hardening; see J. L. Martins and N. Troullier, Phys. Rev. B **46**, 1766 (1992). However, in this case, the site of the alkali atom is an interstitial site between molecules. The intermolecular bonding is very weak at the outset, so that insertion of a foreign atom results in an enhancement of the bonding. We are indebted to S. Saito for pointing this out to us.
[49]H. Dekura, K. Shirai, and A. Yanase, J. Phys.: Conf. Ser. **176**, 012004 (2009).
[50]W. Richter and K. Ploog, Phys. Status Solidi B **68**, 201 (1975).
[51]D. R. Tallant, T. L. Aselage, A. N. Campbell, and D. Emin, Phys. Rev. B **40**, 5649 (1989).
[52]K. Shirai and H. Katayama-Yoshida, J. Phys. Soc. Jpn. **67**, 3801 (1998).
[53]J. L. Hoard, D. B. Sullenger, G. H. L. Kennard, and R. E. Hughes, J. Solid State Chem. **1**, 268 (1970).
[54]B. Callmer, Acta Crystallogr. B **33**, 1951 (1977).
[55]G. A. Slack, C. I. Hejna, and J. S. Kasper, J. Solid State Chem. **76**, 52 (1988).
[56]T. Lundström, in *The International Conference on Boron-Rich Solids*, edited by D. Emin, C. L. Beckel, I. A. Howard, C. Wood, and T. Aselage, AIP Conf. Proc. No. 140 (AIP, New York, 1986), p. 19.
[57]N. Vojteer, J. Stauffer, H. Hillebrecht, K. Hofmann, M. Panda, and B. Albert, Z. Anorg. Allg. Chem. **635**, 653 (2009).
[58]G. D. Watkins, Inst. Phys. Conf. Ser. **23**, 1 (1974).
[59]M. J. Puska, S. Pöykkö, M. Pesola, and R. M. Nieminen, Phys. Rev. B **58**, 1318 (1998).
[60]S. Saito, K. Umemoto, and T. Miyake, in *Fullerene-Based Materials—Structural and Properties, Structure and Bonding*, edited by K. Prassides (Springer, Berlin, 2004), Vol. 109, pp. 41–57.
[61]N. Rey, A. Muñoz, P. Rodríguez-Hernández, and A. S. Miguel, J. Phys. Condens. Matter **20**, 215218 (2008).
[62]M. M. Balakrishnarajan, P. D. Pancharatna, and R. Hoffmann, New J. Chem. **31**, 473 (2007).
[63]R. Car, P. J. Kelly, A. Oshiyama, and S. T. Pantelides, Phys. Rev. Lett. **54**, 360 (1985).
[64]C. S. Nichols, C. G. Van de Walle, and S. T. Pantelides, Phys. Rev. B **40**, 5484 (1989).
[65]K. Shirai, H. Dekura, and A. Yanase, Phys. Status Solidi B **246**, 673 (2009).
[66]K. Shirai, A. Masago, and H. Katayama-Yoshida, Phys. Status Solidi B **244**, 303 (2007).
[67]A. R. Oganov, J. Chen, C. Gatti, Y. Ma, Y. Ma, C. W. Glass, Z. Liu, T. Yu, O. O. Kurakevych, and V. L. Solozhenko, Nature (London) **457**, 863 (2009).
[68]S. Yamanaka, E. Enishi, H. Fukuoka, and M. Yasukawa, Inorg. Chem. **39**, 56 (2000).
[69]E. A. Ekimov, V. A. Sidorov, N. Mel'nik, S. Gierlotka, and A. Presz, J. Mater. Sci. **39**, 4957 (2004).
[70]N. H. Nam, S. Araki, H. Shiraga, S. Kawasaki, and Y. Nozue, J. Magn. Magn. Mater. **310**, 1016 (2007).
[71]P. M. Shirage, K. Miyazawa, H. Kito, H. Eisaki, and A. Iyo, J. Phys. Soc. Jpn. Suppl. C **77**, 40 (2008).